J Electroceram (2010) 25:77–84
DOI 10.1007/s10832-009-9591-x

Textured-Ba(Zr,Ti)O_3 piezoelectric ceramics fabricated by templated grain growth (TGG)

Edward M. Sabolsky · Libeth Maldonado · Matthew M. Seabaugh · Scott L. Swartz

Received: 20 April 2009 / Accepted: 17 September 2009 / Published online: 8 October 2009

Abstract $Ba(Zr_{0.085}Ti_{0.915})O_3$ (BZT) ceramics were grain-oriented (textured) in the <001>-orientation using the Templated Grain Growth (TGG) process. The piezoelectric response of the textured samples was enhanced when poled and measured in the <001>-textured direction. The d_{33}-coefficients for samples measured with a low drive field (<5 kV/cm) displayed values as high as ~975 pC/N. These d_{33}-coefficients were at least three times greater than randomly-oriented BZT ceramics and equally greater than many lead-free piezoelectric ceramics reported in literature. This work successfully demonstrated that grain-oriented BZT ceramics display piezoelectric coefficients (d_{33}-coefficients) that are similar to currently used lead-based materials. This strategy may allow these ceramics to potentially replace some of the lead-based ceramics that are currently being used in various low-temperature and low-drive piezoelectric applications.

Keywords Piezoelectric · Texture · Grain-oriented · Templated grain growth · Lead-free · Barium titanate

E. M. Sabolsky (✉)
Department of Mechanical and Aerospace Engineering,
West Virginia University,
PO Box 6106, Morgantown, WV 26506, USA
e-mail: ed.sabolsky@mail.wvu.edu

L. Maldonado
Laboratoire d'Energétique et de Mécanique
Théorique et Appliquée, Nancy Université,
2 Avenue de la Forêt de Haye—BP 160,
54504 Vandoeuvre lès Nancy Cedex, France

M. M. Seabaugh · S. L. Swartz
NexTech Materials, Ltd.,
404 Enterprise Drive,
Lewis Center, OH 43035, USA

1 Introduction

Piezoelectric ceramics are widely used for electromechanical sensor and transducer applications due to their high generative forces, accurate displacements, and high frequency capabilities. The most commonly used piezoelectric ceramics are solid solutions of lead-based perovskite ceramics, typically a lead zirconate titanate ($Pb(Zr,Ti)O_3$) [1, 2]. $Pb(Zr,Ti)O_3$ (PZT) ceramics show the highest piezoelectric coefficients (d_{33}≈200–600 pC/N) and electromechanical coupling coefficients (k_{33}≈0.6–0.80) of these ceramic compositions.

The future growth of piezoelectric ceramics use in the commercial sector face policy barriers as new environmental laws concerning lead and product disposal are considered. Laws in both Europe and Asia are expected to limit the use of many lead-based compositions, and similar laws may be applied within the United States in the near future. The European Union (EU) Directives on Waste Electrical and Electronic Equipment (WEEE) and Restriction of Hazardous Materials (RHS) declared that many products sold in the European market must be lead-free in the near future [3, 4]. The Japan Electronics and Information Technology Industries Association (JEITA) dictated that many companies will eliminate the use of lead in many of their components and assemblies [5]. These types of restrictions will set barriers to many European and Asian markets, creating a substantial need for new lead-free piezoelectric compositions with properties comparable to lead-based compositions.

Lead-free piezoelectric ceramics typically possess low piezoelectric and electromechanical coupling coefficients (d_{33}<200 pC/N, k_{33}<0.5) relative to PZT compositions [1, 2]. With impending environmental and health laws, there has been a recent surge in research investigating various

lead-free compositions with improved performance. A majority of the work has focused on two perovskite compositions and their various solid solutions, $K_{0.5}Na_{0.5}NbO_3$ (KNN) and $Na_{0.5}Bi_{0.5}TiO_3$ (NBT) [6]. As described by the Zhang et al. review, the performance enhancement of these compositional families originate from the formation of solid solutions within these families that produce either a morphotropic phase boundary (MPB) or polymorphic phase transition. The NBT solid solutions (typically with $K_{0.5}Bi_{0.5}TiO_3$ or $BaTiO_3$) are typically chosen near the MPB that separates the rhombohedral and tetragonal phases. The KNN solid solutions are doped in a manner in which leads to a polymorphic phase transition, where the increased dielectric and piezoelectric performance is dependent upon the increased polarization near temperature related phase transitions. Generally, the performance of these materials are becoming more attractive due their increased piezoelectric coefficients (d_{33}≈180–280 pC/N), reasonable coupling coefficients (k_{33}≈0.59–0.62), and higher Curie temperature (compared to typical $BaTiO_3$ related compositions).

Research has also continued on traditional $BaTiO_3$ compositions. Renewed interest in simple solid solutions of $BaTiO_3$ was initiated due to the work of Rehrig et al. [7] who reported that single crystals of the $Ba(Zr_{0.085}Ti_{0.915})O_3$ (BZT-8.5) composition displayed d_{33}-coefficients >400 pC/N. Rehrig et al. showed that <001>-oriented cuts of rhombohedral $Ba(Zr_{0.085}Ti_{0.915})O_3$ (BZT-8.5) single crystals displayed a low field piezoelectric coefficient (d_{33}) as high as 48 pC/N at room temperature, compared to the d_{33}-coefficient of ~120 pC/N for pure $BaTiO_3$ ceramics. This enhancement was not attributed to doping alone. The enhancement was also attributed to the stable domain configuration in the <001>-poled and -measured state for rhombohedral compositions near to the MPB. Researchers have also shown that single crystals of both rhombohedral $BaTiO_3$ and lead relaxor-$PbTiO_3$ compositions (such as $0.675Pb(Mg_{1/3}Nb_{2/3})O_3$-$0.325PbTiO_3$), when poled and measured in the non-polar <001>, show extraordinary enhancement in the piezoelectric response and electromechanical coupling [8–12]. Yu et al. [8] has also shown that Zr-doped $BaTiO_3$ ($Ba(Ti_{0.92}Zr_{0.08})O_3$ (BZT-8) single crystals oriented in the <001>-direction produce d_{33}-piezoelectric coefficients as high as 850 pC/N. These piezoelectric coefficients are the highest shown for any lead-free material.

Single crystals of lead-free perovskite compositions, such as BZT, are expensive to grow and difficult to manufacture defect-free to large sizes. Randomly-oriented BZT ceramics with a rhombohedral composition do not show the same enhancement as the <001>-oriented single crystals, since the increased piezoelectric performance is dependent upon the <001>-crystallographic direction and the symmetry associated with this direction [13]. Typical ceramics are composed of crystallites (grains), which are randomly-oriented, and therefore display a spherical crystallographic symmetry. With this type of symmetry, the ceramic exhibits an average of its crystallographically dependent properties.

Researchers have shown that dielectric, pyroelectric, and piezoelectric properties become more directionally dependent for ferroelectric ceramic compositions that show a high degree of microstructural texture. Through the manipulation of both the ceramic consolidation and thermal processes, researchers have produced and measured the properties (dielectric and/or piezoelectric) of range of fiber-textured ceramics, which include: $Bi_4Ti_3O_{12}$ [14], $(Sr,Ba)Nb_2O_6$ [15], $(Sr,La)_2Nb_2O_7$ [16], $Sr_2NaNb_5O_{15}$ [17], $PbNb_2O_6$ [18], $(Ba,Bi)TiO_3$ [19], $SrTiO_3$ [20], and solid solutions of NBT [21–24] and KNN [25, 26]. When the fiber-texturing of the grains is in the direction of the polar axis, the piezoelectric and pyroelectric properties were shown to improve drastically due to the increased poling effectiveness. After poling, fiber-textured ceramics show pronounced increases in their dielectric, piezoelectric, and/or pyroelectric properties. Sabolsky et al. [27, 28] were the first to report the texturing of bulk $Pb(Mg_{1/3}Nb_{2/3})$-$PbTiO_3$ (PMN-PT) ceramics, which was later improved upon by other researchers [29, 30]. The formation of <001>-textured PMN-32.5PT ceramics was carried out using the Templated Grain Growth (TGG) processing method. The textured samples showed a two-fold improvement in the strain-field response resulting in low field d_{33} coefficients as high as 1000–1300 pC/N. The piezoelectric response for these works showed low strain-field hysteresis indicating a low degree of loss due to domain movement. This work proved that the crystallographic engineering concept can also be applied to <001>-textured perovskite ceramics with the rhombohedral-tetragonal MPB. Therefore, by texturing ferroelectric ceramics by conventional ceramic processing routes, it is possible to obtain an inexpensive substitute for single crystals that display similar dielectric, pyroelectric, and piezoelectric properties.

Grain-oriented ceramics (textured ceramics) have been produced by various processing means. The development of the texture is usually the result of the orientation and grain growth of aligned anisometric grains. Most of the ferroelectric systems that were uniformly textured to a high degree were fabricated using the TGG process. TGG is a two step process which involves the initial alignment of a small fraction of anisometric seeds (or templates) in a fine-grained matrix due to a high shear force applied during the powder consolidation process (as in processes like tapecasting, extrusion, pressing, and slip casting). In the second step of the process, the green ceramic containing the aligned/oriented particles are thermally processed. During the thermal processing, the ceramic is densified and the

oriented grains begin to grow at the expense of the matrix. This process is typical of exaggerated grain growth, where the growth is driven by the difference in surface free energy between the matrix and the larger template grains. With increasing thermal treatment, the volume fraction of texture increases with an increase of oriented grain growth. The grain growth continues until either grain impingement or driving force reduction due to grain coursening.

The focus of this work was to form <001>-textured Ba $(Zr_XTi_{1-X})O_3$ (BZT) ceramics for future applications in lead-free sensors and transducers. The TGG process was used to orient the BZT grain structure in the <001>-orientation in order to enhance the piezoelectric response of the ceramic when poled and measured in the same direction. A small volume fraction {001}-$SrTiO_3$ platelets were used as templates for the TGG process so that the growth of these templates would impose the <001>-orientation during thermal processing. Most previous piezoelectric research has centered on cation doping strategies in order to alter the physical properties of lead-free ceramics, but this research focused on physically manipulating the ceramic grain orientation to control the directionally dependent properties.

2 Experimental procedure

The $Ba(Zr_{0.085}Ti_{0.915})O_3$ (BZT-8.5) was formed by the conventional solid-state reaction route. The Zr source was obtained by precipitating submicron, hydrous ZrO_2 powder from a $ZrOCl_2$ acid solution (20% Zr content). The dried hydrous ZrO_2 was milled with fumed-TiO_2 (Degussa) and $BaCO_3$ (Alfa-Aesar) in isopropanol for 10 h and then dried. The powder mixture was calcined at 1100°C for 2 h. These procedures produced a single phase, rhombohedral BZT powder with a surface area of ~3.5 m^2/g. The final powder was subsequently milled for a 1 h in isoproponol in order to breakup any hard agglomerates within the powder. The powder was then dried and sieved through 100 mesh. Figure 1 shows a micrograph taken by a scanning electron microscope (SEM) of the resultant BZT powder.

The $SrTiO_3$ platelet particles (NexTech Materials, Ltd.) were synthesized by a molten salt process. Figure 2 shows a SEM micrograph of the perovskite {001}-$SrTiO_3$ platelet particles formed in this work. These particles have an average particle size of ~30–50 μm. The anisotropic shape of these particles allows for easy alignment during the tapecasting and tape lamination.

A slurry containing the BZT-8.5 matrix powder was made with a commercial organic binder system. The platelet $SrTiO_3$ particles (5 vol% of the powder volume) were mixed in the slurry with a magnetic stir bar. The slurry was cast with a blade height of ~250 μm at a shear rate of ~350 s^{-1}. The tapes were dried, cut, and were laminated at 80°C in an isostatic laminating press. The final green laminated samples displayed a thickness ~1 mm, and were cut to an area of ~2×2 cm with a hot razor-blade. The green laminates were burned out at 600°C in air. The burned-out samples were thermally treated at temperatures between 1300–1400°C for 1–10 h in air. The large area of the samples was polished with diamond paste to a 6 μm finish, and XRD and density measurements were then completed on the samples. The <001>-texture fraction was estimated by the Lotgering method [31]. As stated in previous papers, the Lotgering factor is considered to be an estimation of the volume fraction of textured material. The texture fraction typically varies across the volume of the samples due to the template particle positional and orientation distribution. In this work, multiple XRD patterns at various depths through the sample thickness, and the reported the Lotgering factor

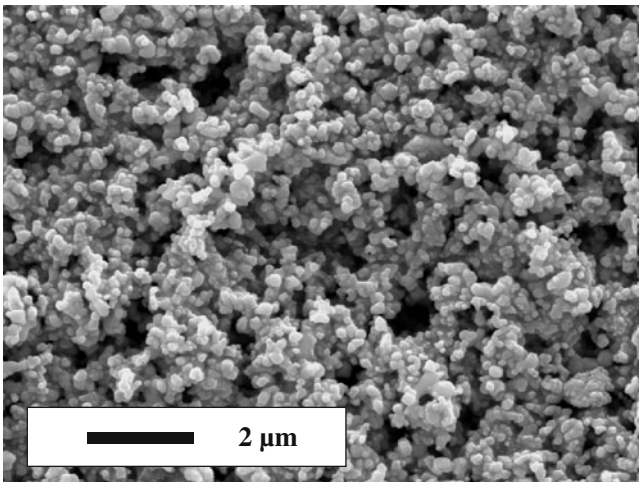

Fig. 1 Scanning electron micrograph displaying random BZT-8.5 matrix powder used in TGG process

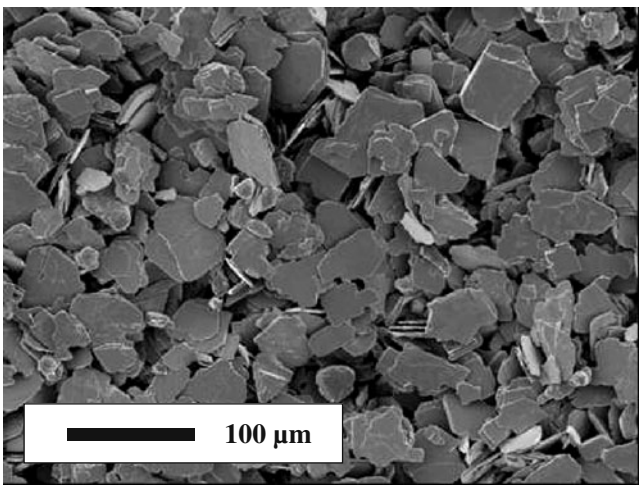

Fig. 2 Scanning electron micrograph displaying the {001}-$SrTiO_3$ platelet particles used as templates in the TGG process

is calculated and averaged over these XRD patterns to account for some of the inhomogeneity.

The low field dielectric constant (and loss) was measured as a function of temperature with a multi-frequency impedance meter (HP 4284A LCR meter) combined with a temperature regulated oven. The BZT-8.5 samples were electroded with Au/Pd by sputtering. The dielectric constant and loss were measured on poled samples between −25–200°C and over a frequency range of 1 kHz–100 kHz during heating. The BZT samples were poled with a DC-bias of 30 kV/cm for 15 min at room temperature in polydimethylsiloxane (Dow Corning 200 Fluid).

Both the dielectric polarization versus electric field measurements (P-E hysteresis loops) and the unipolar strain versus electric field measurements (strain-field curves) were completed using a modified Sawyer-Tower circuit. The unipolar strain versus electric field measurements (strain-field curves) were measured using the Sawyer-Tower circuit in conjunction with a linear variable differential transducer, driven by a lock-in amplifier (Standford Research Systems, Model SR830). The required high fields were generated by a Trek 609C-6 high-voltage amplifier. The strain and polarization of the samples were measured while immersed in Galden HT-200 to prevent arcing. The low-field piezoelectric coefficients (d_{33}) for the samples were estimated from the slope of the unipolar strain-field curves.

3 Results and discussion

3.1 Templated grain growth of BZT ceramics

Figure 3 displays the x-ray diffraction (XRD) patterns of the BZT-8.5 ceramic samples containing 5 vol% $SrTiO_3$ template particles. The XRD pattern was taken from the surface parallel to the <001>-oriented template alignment. The samples were sintered at 1320–1350°C for 2–10 h, and all sampled displayed densities of ~97% (5.95 g/cc theoretical). Templated samples that were sintered at <1320°C or >1350°C displayed densities ranging between 70–90% of theoretical density.

The XRD pattern for dense, randomly-oriented BZT-8.5 ceramic (containing no $SrTiO_3$ templates) was added to Fig. 3 for comparison. The randomly-oriented BZT-8.5 ceramic shows that the (110) peak is the highest intensity peak for the rhombohedral, perovskite BZT-8.5 composition. The figure shows that by sintering the templated samples between 1275–1350°C, the <001> peaks increased in intensity while all other (hkl) peaks decreased in intensity. The XRD patterns of the BZT-8.5 sample seemed to be independent of sintering time when processed between 1320–1350°C, meaning that the grain size saturates quickly at these temperatures. The peak intensity change represents an increase in the volume fraction of <001>-texture. The degree of <001>-texture can be estimated by using the Lotgering relation [31]. The Lotgering factor (f) is defined as the area fraction of textured material in the [hkl] of interest.

The templated samples in this work showed extraordinary growth kinetics at the temperatures processed. The BZT-8.5 ceramics were textured within the first 2 h of annealing at 1320–1350°C. The XRD of the templated BZT-8.5 ceramics sintered at 1350°C showed >90% texturing (f>0.9). Again, regardless of the length of sintering time (2–10 h), the templated samples all showed a similar degree of texturing. The kinetics for grain growth at these temperatures was extensive and grain impingement occurred very quickly. Future work will focus on the mechanism and kinetics of the nucleation and growth process within this templated system. The XRD pattern of the textured ceramics show only a single peak at the {00l} position, indicating that the textured ceramic possesses the

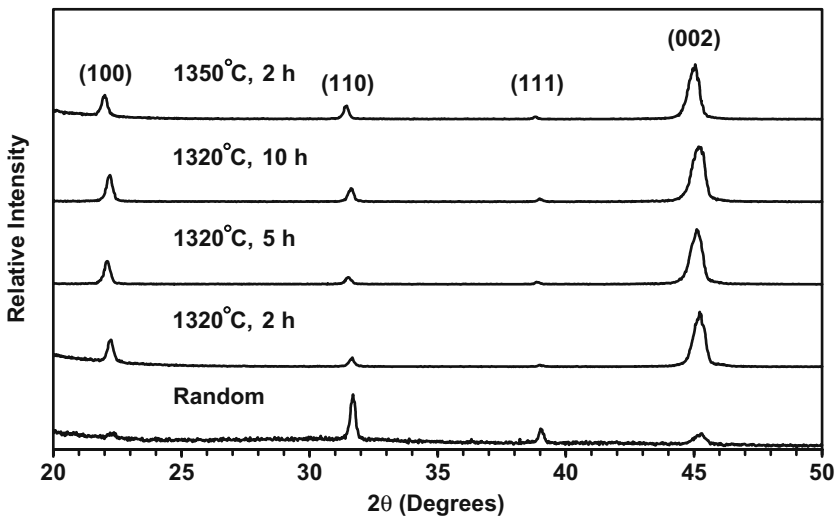

Fig. 3 XRD pattern of random and textured BZT-8.5 ceramics containing 5 vol% oriented {001}-$SrTiO_3$ templates annealed at 1320–1350°C for 2–10 h

appropriate (and desired in this case) rhombohedral crystal structure.

3.2 Dielectric properties of un-textured and textured BZT ceramics

The dielectric properties of the random BZT-8.5 ceramic were measured in order to compare and contrast the results obtained for the textured-BZT ceramics. The properties obtained for these random samples were considered as the baseline values in order to highlight the effect of texturing on the BZT-8.5 composition. The properties for the random samples were measured using the same equipment and procedure as the textured samples.

Figure 4 displays the dielectric constant as a function of temperature for a poled, randomly-oriented BZT-8.5 ceramic. The sample shows two anomalies in its dielectric-temperature response. The first anomaly at is at ~60°C, and this temperature represents the phase transition between the ferroelectric rhombohedral and tetragonal phases. It is well established by previous researchers that the addition of Zr as a dopant in $BaTiO_3$ results in the "pinching" of the phase transitions [2]. "Pinching" refers to the temperature increase for the rhombohedral-orthorhombic and the orthorhombic-tetragonal transitions, with a decrease in the tetragonal-cubic transition (T_C). At the 8.5 mol% Zr composition, the rhombohedral-orthorhombic and the orthorhombic-tetragonal transitions merge into a single transition area (T_{r-t}) where all three phases are thermodynamically probable. The T_{r-t} and T_C measured for the BZT ceramic formed in this work were 60°C and 95°C, respectively, which was similar to the results measured by both Yu et al. and Dobal et al. [32]. Irregular features can also be seen in the dielectric patterns near ~40°C, but a definite transition can not be resolved and does not match transitions previously identified by other researchers. The measured ε_{r-t} and ε_{max} were 2,300 and 11,300, respectively. These values are much lower than the values reported by Dobal et al. for BZT-8 ceramics. Dobal et al. reported ε_{r-t} and ε_{max} as high as 4,000 and 31,000, respectively. The lower than expected dielectric constants may be the result of ~3 vol% residual porosity which remained in the random BZT ceramics. Porosity has large effect on the dielectric constant of a material without drastically altering the transition temperatures. Dobal et al. did not report the density of the BZT-8 ceramics, so an absolute comparison between properties and density can not be made with this work. The added features within the dielectric data may indicate chemical inhomogeneity resulting in decreased dielectric performance. Further characterization of processing-property relationships will be required in future work on this system.

Figure 5 displays the dielectric constant as a function of temperature for >90%-textured BZT-8.5 ceramic (5 vol% $SrTiO_3$ platelet templates). The density of the textured samples was similar to that for the un-textured samples (~97% density). The phase transition temperatures were unaltered by the addition of the $SrTiO_3$ template particles, which may indicate that minimal amounts of $SrTiO_3$ dissolved into the matrix material. Sr additions into $BaTiO_3$ are well known to result in a decrease in the transition temperatures. The ε_{r-t} and ε_{max} for the textured samples were 2,100 and 8,000, respectively. Similar to the results obtained by Rehrig et al. [7] for the <001>-oriented BZT-8.5 single crystals, the dielectric constant of the textured ceramics decreased when measured in the poled <001>-orientation. Rehrig et al. reported $\varepsilon_{rt} \approx 2{,}000$ and $\varepsilon_{max} \approx 18{,}000$ for <001>-oriented single crystals, which is lower than that predicted for a single crystal oriented and measured at an angle from the dipole direction (the <111>-direction). Rehrig et al. did not suggest a cause for the lower than expected dielectric constant. The textured samples within

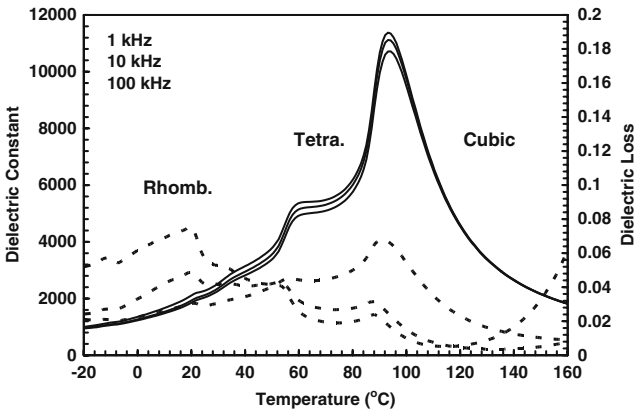

Fig. 4 Dielectric constant and loss as a function of temperature for poled, random BZT-8.5 ceramics containing 0 vol% $SrTiO_3$ templates

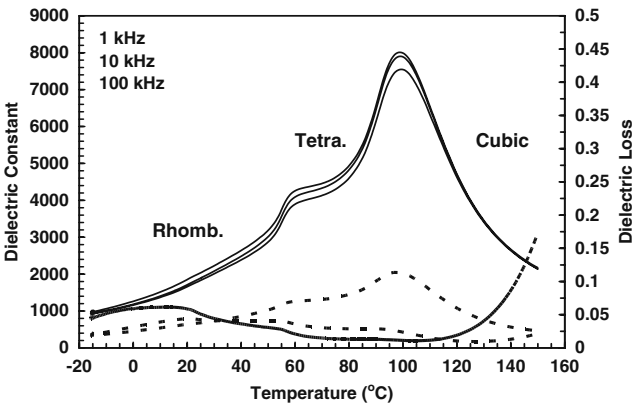

Fig. 5 Dielectric constant and loss as a function of temperature for poled, 90%-textured BZT-8.5 ceramics containing 5 vol% $SrTiO_3$ templates

this work have both the residual porosity and the remaining $SrTiO_3$ phase to attribute to the decreased permittivity.

The dielectric polarization as a function of bipolar electric field was measured for random BZT-8.5 and <001>-textured BZT (5 vol% $SrTiO_3$). The textured sample was measured in the <001>-oriented direction. Figure 6 shows the ferroelectric polarization-field response for both samples. The random BZT-8.5 ceramic composition showed a $P_r \approx 5.9$ μC/cm^2 and $E_c \approx 2.0$ kV/cm. The textured BZT-8.5 ceramic showed an increase in both the remanent polarization and the coercive field ($P_r \approx$ 11.0 μC/cm^2, $E_c \approx 5.0$ kV/cm) over the behavior of the random BZT-8.5 ceramic. For reference to oriented single crystals, Yu et al. and Rehrig et al. showed that <001>-oriented BZT crystals have a $P_r \approx 10$–15 μC/cm^2, $E_c \approx$ 2.5 kV/cm. The increase in the remanent polarization cannot be attributed to the <001>-texturing, since the ceramic is oriented and tested in the non-polar direction; and therefore, the measured polarization should be smaller (up to a factor of $\sqrt{3}$) than the polarization vector magnitude. The discrepancy in the polarization data may be related to the residual $SrTiO_3$ phase and its effect on the dielectric, ferroelectric/ferroelastic, and piezoelectric properties of the effective composite. Since $SrTiO_3$ has a smaller dielectric constant compared to the BZT composition, it can be assumed that the there would be a significant field concentration around these inclusions affecting the poling efficiency, dielectric and electromechanical responses. In addition, the presence of the non-piezoelectric $SrTiO_3$ within the BZT grains would clamp the piezoelectric response of the composite grains. Through a simplified finite element analysis (FEA) model, Messing et al. [33] showed that for a textured ceramic composite of $BaTiO_3$ and PMN-PT, the presence of residual $BaTiO_3$ within the PMN-PT could result in very high local strains and stresses around these intragranular inclusions (~0.38% and 8 MPa, respectively). These high stresses may locally destabilize the rhombohedral phase and force a local phase transition to the orthorhombic or tetragonal structures. This local stress-induced phase transformation, especially to the tetragonal structure, may account for the increase in the apparent remanent polarization for the <001>-textured BZT-8.5 ceramics. Similar to this work, other piezoelectric TGG studies using a heteroepitaxial seeding (or templating) process have expressed similar concern with the effect of the residual template particles on the final properties. Further investigation and modeling is needed in this area.

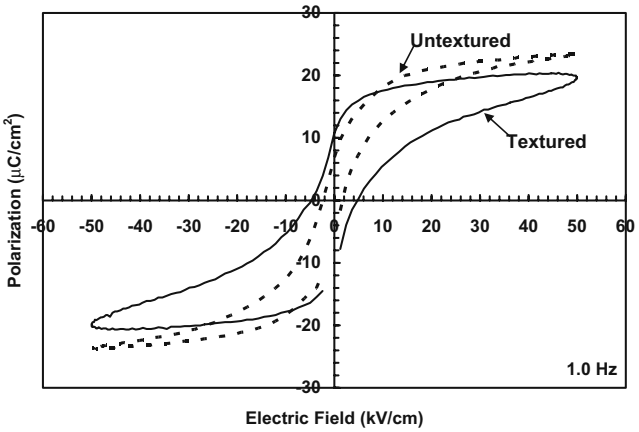

Fig. 6 Polarization-electric field hysteresis for un-textured (0 vol% $SrTiO_3$ templates) and 90%-textured BZT-8.5 ceramic containing 5 vol% $SrTiO_3$ templates

3.3 Piezoelectric properties of un-textured and textured BZT ceramics

The strain-field data was collected by a linear variable differential transducer in conjunction with the Sawyer-Tower circuit. The field was applied at a frequency of 0.2 Hz and the strain-field data was continuously collected over the course of the measurement. The d_{33}-coefficients can be measured from the slope of the strain-field plots for fields under <5 kV/cm. The opening of the strain-field trend was also monitored in order to characterize the extrinsic contribution to the piezoelectric response. The piezoelectric coefficient can be affected by the piezoelectric hysteresis, which adds to the intrinsic strain response of the material. The hysteresis (extrinsic strain) is a result of domain wall motion due to non-stable domain configurations. The strain due to extrinsic domain movement contributions is not usable or desirable in most piezoelectric applications. A qualitative estimation of the degree of piezoelectric hysteresis can be completed by measuring difference between the strain level on the application and release of the field at a singular field value.

The strain-field behavior of random (un-textured) BZT-8.5 and >90%-textured BZT ceramics is shown in Fig. 7. The figure shows that the random BZT-8.5 ceramic displayed a maximum strain output of ~0.13% (at 50 kV/cm) and a low field d_{33}-coefficient of ~300 pC/N. The measured d_{33}-coefficient is slightly higher than that reported in literature ($d_{33} \approx 250$–300 pC/N). The highly, textured BZT ceramic produced a strain output of ~0.19% at 50 kV/cm. The highly textured BZT samples showed relatively little opening, or piezoelectric hysteresis, in the strain-field curves (<0.02%). The d_{33}-coefficients can be measured from the slope of the strain-field plots for fields under <5 kV/cm. The low piezoelectric hysteresis indicates that the strain level and piezoelectric coefficient are not inflated due to the relatively unusable strain produced by domain wall movement within the sample. The piezoelectric hysteresis is at least half of that reported by Yu et al. for their BZT single crystals and

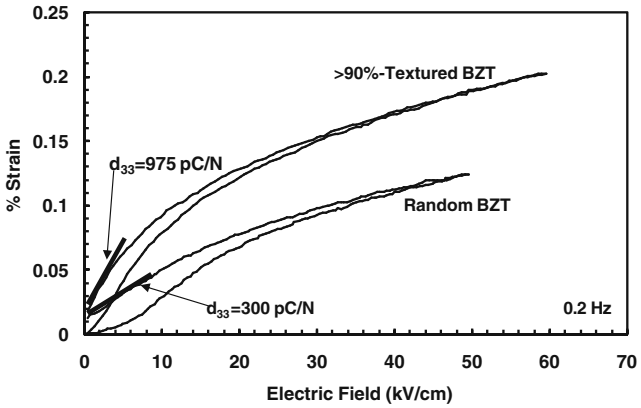

Fig. 7 Unipolar strain-electric field curves (measured at 0.2 Hz) of random BZT-8.5 (containing 0 vol% $SrTiO_3$ templates) and textured BZT-8.5 (containing 5 vol% $SrTiO_3$ templates)

polycrystalline ceramics. The low-field d_{33} coefficient (<5 kV/cm) for samples with ~90% texture was in the range of ~975 pC/N. Piezoelectric coefficients of this magnitude are at least three times greater than that measured for a randomly-oriented BZT ceramic.

Figure 8 shows the unipolar strain-field response of textured BZT-8.5 and $0.675Pb(Mg_{1/3}Nb_{2/3})O_3$-$0.325PbTiO_3$ (PMN-32.5PT) on the same plot. The PMN-32.5PT ceramic composition is considered a soft ferroelectric, and it is comparable to many of the soft PZT compositions. The d_{33} (at low fields, <5 kV/cm) of random PMN-32.5PT ceramics is typically between 650–700 pC/N, as was measured and presented in Fig. 8. Figure 8 shows that the strain-field response of the highly textured BZT-8.5 is similar, or even slightly larger, to the response of PMN-32.5PT random ceramic. The figure boldly demonstrates that the <001>-texturing of the rhombohedral BZT-8.5 composition significantly improves the piezoelectric response of this lead-free ceramic up to a level similar to soft PZT and PMN-PT random ceramics. The textured BZT-8.5 ceramics are performing beyond any lead-free ceramic reported, and the

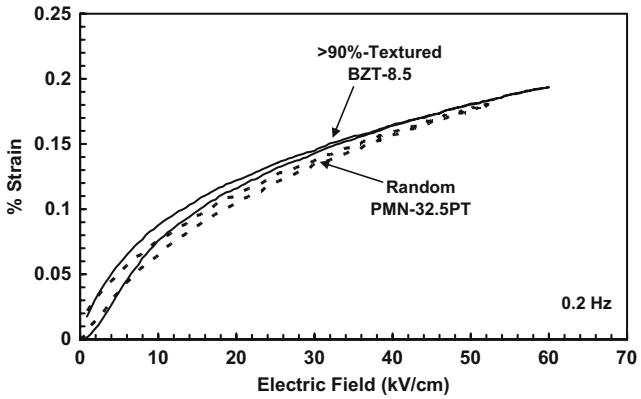

Fig. 8 Comparison of the unipolar strain-electric field trends of ~90%-textured BZT-8.5 and a random PMN-32.5PT ceramic measured at 0.2 Hz

d_{33}-coefficient of the textured BZT-8.5 is near to that of the various PZT ceramics. Also, the textured BZT-8.5 ceramics are approaching the performance that was attained for <001>-oriented BZT-8.5 single crystals, which show the highest piezoelectric performance of a lead-free material. Unfortunately, the BZT-8.5 compositions has a large negative quality; the BZT-8.5 composition has a relatively low Curie temperature, which means that the application of this composition is limited to uses at or below ~60°C (the rhombohedral-tetragonal phase transition). As the temperature approaches the various phase transitions ≥60°C, the sample will de-pole from the <111>-orientation and the benefits achieved through domain engineering will be lost. Thus, the textured BZT-8.5 ceramics developed in this work can only be applied to applications at lower temperatures, but this still provides ample opportunity to potentially replace some lead-based ceramics that are currently being used in various low-field applications.

4 Conclusions

BZT-8.5 ceramics were fiber-textured in the <001> by the TGG process using {001}-$SrTiO_3$ template particles. XRD was completed on the surface perpendicular to the oriented $SrTiO_3$ platelet particles, and templated BZT-8.5 ceramics showed >90% texturing (f>0.9) for sintering temperatures between 1320–1350°C. Regardless of the incorporation of the $SrTiO_3$ within the BZT material, the XRD pattern of the textured ceramics showed only a single peak at the {00l} position, indicating that the appropriate rhombohedral crystal structure was retained regardless of potential solid solution formation or clamping effects.

The dielectric constant as a function of temperature for the textured BZT-8.5 ceramics showed a similar response to that of a random, untemplated BZT ceramic. The phase transition temperatures were unaltered by the addition of the $SrTiO_3$ template particles. The texture had a significant effect on the piezoelectric performance. The average d_{33}-piezoelectric coefficients of the highly textured BZT-8.5 ceramics were at least three times greater than randomly-oriented samples containing no $SrTiO_3$ templates. Also, the piezoelectric response showed a high linear trend in the low field regime indicating minimal piezoelectric hysteresis.

Acknowledgements The authors would like to acknowledge the financial support from the National Science Foundation (Contract No. DMI-0349673), West Virginia University Research Corporation, and WVU College of Engineering and Mineral Resources. The authors would also like to thank Jeff Long of the Materials Research Institute at the Pennsylvania State University for his assistance with the strain-field and dielectric measurements.

References

1. G. Haertling, J. Am. Ceram. Soc. **82**, 797 (1999)
2. B. Jaffe et al., *Piezoelectric ceramics* (Academic, New York, 1971), p. 92
3. Directive 2002/96/EC of the European Parliament and Council on waste and electrical and electronic equipment (WEEE).
4. Directive 2002/95/EC of the European Parliament and Council on the restriction of the use of certain hazardous substances in electrical and electronic equipment (RHS).
5. Lead-free Roadmap V1.3 for commercialization of lead-free solder and components, Japan Electronics and Information Technology Industries Association (2002).
6. S. Zhang, R. Xia, R. Shrout, J. Electroceram. **19**, 251 (2007)
7. P. Rehrig, S.E. Park, S. Trolier-McKinstry, G.L. Messing, B. Jones, T.R. Shrout, J. Appl. Phys. **86**, 1657 (1999)
8. Z. Yu, R.Y. Guo, A.S. Bhalla, Matt Lett. **57**, 349 (2002)
9. S. Wada, H. Adachi, H. Kakemoto, H. Chazono, Y. Mizuno, H. Kishi, T. Tsurumi, J. Mater. Res. **17**, 456 (2002)
10. T. Tsurumi, Y. Yamamoto, H. Kakemoto, S. Wada, H. Chazono, H. Kishi, J. Mater. Res. **17**, 755 (2002)
11. S.-E. Park, S. Wada, L.E. Cross, T.R. Shrout, J. Appl. Phys. **86**, 2746 (1999)
12. S.-E. Park, T.R. Shrout, J. Appl. Phys **82**, 1804 (1997)
13. Y. Avrahami, H.L. Tuller, J. Electroceram. **13**, 463 (2004)
14. S.-H. Hong, S. Trolier-McKinstry, G.L. Messing, J. Am. Ceram. Soc. **83**, 113 (2000)
15. C. Duran, S. Trolier-McKinstry, G.L. Messing, J. Am. Ceram. Soc. **83**, 2203 (2000)
16. B. Brahmaroutu, *Templated grain growth of textured strontium niobate ceramics*. Ph.D. Thesis, Pennsylvania State University, University Park, PA (1999).
17. Y. Doshida, H. Kishi, Y. Hattori, A. Makiya, S. Tanaka, K. Uematsu, and T. Kimura, *12th US-Japan seminar on dielectric and piezoelectric ceramics* (ed.), C. Wu, H. Kishi, C. Randall, P. Pinceloup, H. Funakubo, (Maryland, 2005), p. 123.
18. M. Granahan, J. Am. Ceram. Soc. **64**, C68 (1981)
19. T. Sugawara, M. Simizu, T. Kimura, K. Takatori, T. Tani, Ceram. Trans. **136**, 389 (2003)
20. T. Takeuchi, T. Tani, J. Ceram. Soc. Japan **110**, 232 (2002)
21. H. Yilmaz, G.L. Messing, S. Trolier-McKinstry, J. Electroceram. **11**, 207 (2003)
22. T. Tani, J. Korean Phys. Soc. **32**, S1217 (1998)
23. T. Kumara, E. Fukuchi, T. Tani, Jpn. J. Appl. Phys. **44**, 8055 (2005)
24. E. Fukuchi, T. Kimura, T. Tani, T. Takeuchi, Y. Saito, J. Am. Ceram. Soc. **85**, 1461 (2002)
25. Y. Saito, H. Takao, T. Tani, T. Nonoyama, K. Takatori, T. Homma, T. Nagaya, M. Nakamura, Nature **432**, 84 (2004)
26. T. Tani, T. Kimura, Adv. Appl. Ceram. **105**, 55 (2006)
27. E.M. Sabolsky, A.R. James, S. Kwon, S. Trolier-McKinstry, G.L. Messing, Appl. Phys. Lett. **78**, 2551 (2001)
28. E.M. Sabolsky, S. Trolier-McKinstry, G.L. Messing, J. Appl. Phys. **93**, 4072 (2003)
29. K.H. Brosnan, G.L. Messing, R.J. Meyer, M.D. Vaudin, J. Am. Ceram. Soc. **89**, 1965 (2006)
30. T. Richter, S. Denneler, C. Schuh, E. Suvaci, R. Moos, J. Am. Ceram. Soc. **91**, 923 (2008)
31. F.K. Lotgering, J. Inorg. Nucl. Chem. **9**, 113 (1959)
32. P.S. Dobal, A. Dixit, R.S. Katiyar, Z. Yu, R. Guo, A.S. Bhalla, J. Appl. Phys. **89**, 8085 (2001)
33. G.L. Messing, S. Trolier-McKinstry, E.M. Sabolsky, C. Duran, S. Kwon, B. Brahmaroutu, P. Park, H. Yilmaz, P.W. Rehrig, K.B. Eitel, E. Suvaci, M. Seabaugh, K.S. Oh, Crit. Rev. Sol. St. Mat. Sci. **29**, 45 (2004)